# Model for classical and ultimate regimes of radiatively driven turbulent convection.

Mathieu Creyssels

# Model for classical and ultimate regimes of radiatively driven turbulent convection

**M. Creyssels†**

Laboratoire de Mécanique des Fluides et d'Acoustique, Ecole Centrale de Lyon, Univ. Lyon, CNRS, 69134 Ecully, France

(Received xx; revised xx; accepted xx)

In a standard Rayleigh-Bénard experiment, a layer of fluid is confined between two horizontal plates and the convection regime is controlled by the temperature difference between the hot lower plate and the cold upper plate. The effect of direct heat injection into the fluid layer itself, for example by light absorption, is studied here theoretically. In this case, the Nusselt number ($Nu$) depends on two non-dimensional parameters: the Rayleigh number ($Ra$) and the ratio between the spatial extension of the heat source ($l$) and the height of the fluid layer ($h$). For both the well-known classical and ultimate convection regimes, the theory developed here gives an analytical formula for the variations of the Nusselt number as a function of $Ra$ and the $l/h$ ratio. For large Rayleigh numbers and in the classical convection regime, by increasing $l/h$ from 0 to 1/2, the $Ra$-dependent Nusselt number gradually changes from the standard scaling $Nu \sim Ra^{1/3}$ to the asymptotic scaling $Nu \sim Ra^{2/3}$. For the ultimate convection regime, $Nu$ gradually changes from $Nu \sim Ra^{1/2}$ scaling to an asymptotic behaviour seen only at very high Ra for which $Nu \sim Ra^2$. This theory is validated by the recent experimental results given by Bouillaut *et al.* (2019), at least in the classical regime. The predictions for the ultimate regime cannot be confirmed at this time due to the absence of experimental or numerical works on Rayleigh-Bénard convection both driven by internal sources and for very large $Ra$.

## 1. Introduction

Rayleigh-Bénard (RB) convection is a classical fluid dynamics problem and has been the subject of numerous experimental, theoretical and numerical studies. When Rayleigh numbers are very high (generally above $10^6$), two distinct theories, called classical and ultimate, give two distinct asymptotic behaviours for the Nusselt number as a function of the Rayleigh number. The classical theory states that the heat flux should be independent of the height of the fluid layer leading from the definition of $Nu$ and $Ra$ to the following asymptotic law: $Nu \sim Ra^{1/3}$. The ultimate theory asserts that for very high Rayleigh numbers, the heat flux should become independent of the fluid dissipative coefficients $\nu$ and $\kappa$ giving an asymptotic law like $Nu \sim Ra^{1/2}$ (Kraichnan 1962; Siggia 1994; Chavanne *et al.* 1997; Ahlers *et al.* 2009; Chillà & Schumacher 2012).

This paper is an extension of these two theories of convection in the case of a heat source spatially distributed within the fluid layer. An example of this kind of heating is given by Lepot *et al.* (2018); Bouillaut *et al.* (2019). The authors experimentally developed a new RB cell concept for which heat is not injected through thermal conduction between the lower heating plate and the fluid above it. In their experiment, the lower plate is transparent and the working fluid is a homogeneous mixture of water and dye. A powerful

† Email address for correspondence: mathieu.creyssels@ec-lyon.fr

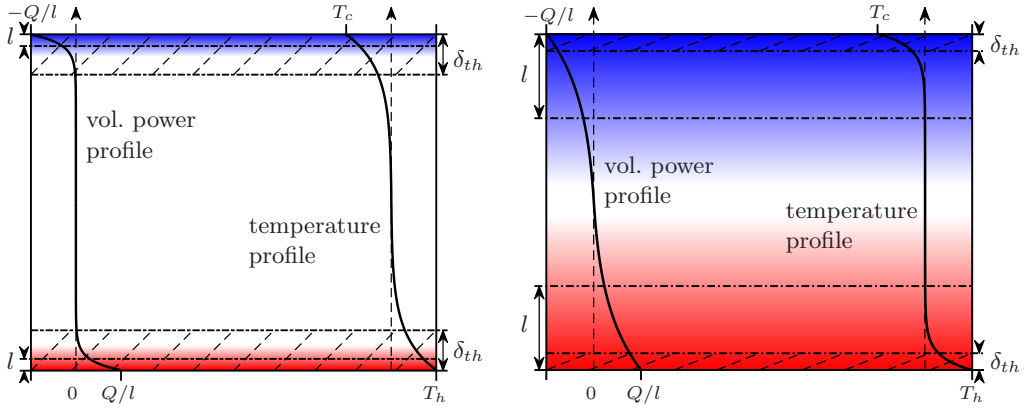


FIGURE 1. Modified RB experiment in the case of $l/\delta_{th} < 1$ (left) and in the case of $l/\delta_{th} > 1$ (right). The heat is injected in volume near the lower plate (red zone) while the fluid is cooled in volume near the upper plate (blue area), both with a characteristic length $l$. The two thermal boundary layers with a width of $\delta_{th}$ are also displayed (hatched areas). The profile of the volumetric (positive and negative) power source and the temperature profile are also shown for each case.

spotlight placed under the lower plate shines through the fluid, and the light, after passing through the transparent plate, is absorbed by dye and therefore by the fluid located near the plate. According to the Beer-Lambert law, this kind of heating corresponds to a volume heat source that decays exponentially from the lower plate to a characteristic height $l$, leading to a local heating of the following form:

$$q_v(z) = \frac{Q}{l} \exp\left(-\frac{z}{l}\right), \tag{1.1}$$

where $Q$ is the total heat flux radiated by the spotlight into the fluid (in $\mathrm{W/m^2}$) and $z$ is the vertical coordinate with $z = 0$ on the lower plate. The characteristic height $l$ can be changed since it is inversely proportional to the dye concentration. Hereafter, (1.1) is assumed to be valid even if the model proposed in this article can easily be generalized to other forms of local heating rates.

Lepot *et al.* (2018); Bouillaut *et al.* (2019) and Doering (2019) showed that the study of this type of modified RB experiments should allow progress in understanding turbulent convection in both natural flows and a conventional RB cell. Indeed, in many geophysical and astrophysical flows, convection is driven by internal heating due to, for example, the radioactive decay in the Earth's mantle or the thermonuclear reactions in stars. It is therefore easy to understand that a modified RB experiment is a first approach to model turbulent flows in natural systems even if $Ra$ numbers are very different. In addition this work also aims to provide interesting information on turbulent convection. Indeed, heat transport in a conventional RB cell is essentially controlled by the thermal boundary layers near the plates and their stability explains the difference between the two theories of convection (the classical and the ultimate). To investigate these boundary layers, the location of heat sources can be easily changed by adjusting the absorption height $l$ (Lepot *et al.* 2018; Bouillaut *et al.* 2019). This is a similar approach to that used by other authors, which consists of replacing the lower and upper plates with rough plates (Shen *et al.* 1996; Roche *et al.* 2001; Qiu *et al.* 2005; Stringano *et al.* 2006; Tisserand *et al.* 2011). Roche *et al.* (2001) and Tisserand *et al.* (2011) reported an increase of the $Nu$ vs $Ra$ scaling exponent from 1/3 to 1/2, even if the range of $Ra$ explored and their interpretation of it was very different. Roche *et al.* (2001) interpreted the transition for the exponent to

the value 1/2 as a turbulent transition for the thermal boundary layers because the $Ra$ numbers were high ($> 10^{12}$) and the transition was already observed with smooth plates. On the contrary, Tisserand *et al.* (2011) interpreted the increase in the exponent as a destabilization by buoyancy of the fluid placed between the rough elements.

In this theoretical study, a model is proposed to deduce scaling laws of the Nusselt number as a function of the two non-dimensional parameters that control turbulent convection *i.e.* the Rayleigh number and the ratio of absorption height to cell height ($\tilde{l} = l/h$). In a standard RB experiment, both plates play the same role (for a small temperature difference and by adopting the Boussinesq approximation) and the corresponding thermal boundary layers have the same behaviour and therefore the same width ($\delta_{th}$). To have two similar boundary layers in a modified RB cell, the upper part of the cell must be cooled with the same power profile as that used for the heating process, so $q_v(z) = -\frac{Q}{l}\exp(-\frac{h-z}{l})$. The injected or extracted power profile is shown in Fig. 1 for both cases $l/\delta_{th} < 1$ (left) and $l/\delta_{th} > 1$ (right). When $l \to 0$, this experiment becomes a standard RB experiment while, when the length $l$ increases, the lower and upper thermal boundary layers are heated and cooled respectively. Finally, when $l$ becomes greater than $\delta_{th}$, the bulk flow is also heated and cooled simultaneously since the lower region is heated while the upper region is cooled (Fig. 1 right). The Rayleigh number in a modified RB experiment can be defined as in a conventional RB cell by using the temperature difference between the two plates ($\Delta T = T_h - T_c$), between the lower plate and the mean bulk flow ($\Delta T = 2(T_h - T_b)$) or between the mean bulk flow and the upper plate ($\Delta T = 2(T_b - T_c)$). When Rayleigh numbers are high, it is assumed that the convective flow of a modified RB experiment is strong enough to impose an almost constant mean temperature over time in the bulk flow, *i.e.* outside the boundary layers (see Fig. 1), as experimentally observed in a standard RB experiment.

A major difference between the modified RB experiments and the standard RB experiments concerns the mean heat flux through the cell from the bottom plate to the top plate. Indeed, when a steady state is reached, the heat flux averaged over a horizontal section must be independent of the vertical coordinate ($z$) for a standard RB experiment, whereas for a modified RB cell, this heat flux cannot be constant even in a steady state. When considering a horizontal slice of fluid, the energy given in volume must be evacuated outside the slice, which requires a gradient of the mean heat flux in the fluid. However, unlike the standard RB case, the two horizontal plates and the side walls are assumed to be perfectly insulated to prevent heat transfer, and to lead to the same heat flux inside the fluid ($Q\vec{e}_z$) at both the lower and upper plate ($z = 0$ and $z = h$). Far from the plates, for example in the center of the cell where $l \ll z \ll h - l$, the volumetric heat source $q_v$ is close to 0, and energy conservation leads to a heat flux also equal to $Q\vec{e}_z$. Thus, with the exception of the blue and red regions shown in Fig. 1, $Q$ represents the heat flux through the cell and the Nusselt number can be defined as in a standard RB experiment as

$$Nu = \frac{Qh}{\lambda \Delta T}, \tag{1.2}$$

where $\lambda$ is the thermal conductivity of the fluid and $h$ the height of the cell. As previously mentioned, when $l \to 0$, $Nu$ tends towards the Nusselt number that can be obtained in the same cell but with standard RB conditions that are a constant heat flux and fixed temperatures at both plates. Hereafter, this Nusselt number will be taken as a reference and called $Nu_0(Ra) = \lim_{l\to 0} Nu(Ra, l)$.

Finally, it is questionable whether this type of modified RB experiment can be performed experimentally. Indeed, heating in volume can be achieved using either strong

light (Lepot *et al.* (2018)), an electric current or even by fixing heating elements in the fluid (Kulacki & Goldstein (1972); Goluskin (2015); Goluskin & van der Poel (2016)). On the contrary, cooling in volume is more difficult to achieve experimentally. However, Lepot *et al.* (2018); Bouillaut *et al.* (2019) have shown that, in their experiments, turbulent convection develops quasi-stationary internal temperature gradients leading to a temperature difference between the lower plate and the bulk flow that is almost constant over time (see Fig. 1 B in Lepot *et al.* (2018)). Therefore, the theoretical results given below will be compared in section 4 with those obtained experimentally by Lepot *et al.* (2018); Bouillaut *et al.* (2019). The theoretical model is based on the known structure of the flow and temperature fields observed experimentally and numerically in a standard RB cell at high Rayleigh numbers (generally $> 10^5$).

## 2. Background on $Nu$ vs $Ra$ scalings for standard RB convection

For high Rayleigh numbers, convective flow is heavily turbulent almost everywhere in the cell except in two thin thermal boundary layers located against the lower and upper plates. This dynamic structure of the flow yields to a particular field for the mean temperature. Indeed, in the bulk flow, turbulent convection produces large temporal and spatial variations for temperature fluctuations but an almost uniform mean temperature field with $\overline{T}_b = (T_h + T_c)/2$ for symmetry reasons and assuming the Boussinesq approximation is valid (the mean temperature profile is represented in Fig. 1). On the contrary, the mean temperature increases or decreases by $\Delta T/2 = (T_h - T_c)/2$ in each boundary layer. Therefore, the heat transfer averaged over an horizontal section is dominated by turbulent convection in the bulk flow ($\overline{\Phi} \approx \rho c_p \overline{w'T'}$, where $w'$ and $T'$ are the fluctuations of the vertical velocity and temperature respectively), whereas the heat transfer is driven by thermal conduction in the two thin boundary layers ($\overline{\Phi} \approx -\lambda \partial \overline{T}/\partial z$, where $\overline{T}(z)$ is the temperature averaged both on time and on an horizontal section located at the distance $z$ from the plate). The thickness of each thermal boundary layer ($\delta_{th}$) is controlled by the temperature difference $\Delta T/2$ and the mean heat flux assuming that $\overline{\Phi}$ can be written as $\overline{\Phi} = \lambda \Delta T/(2\delta_{th})$. This last equation is valid regardless of the convection regime (classical or ultimate, see Kraichnan (1962)) leading to a ratio $\delta_{th}/h$ depending only on the Rayleigh number as

$$\frac{\delta_{th}}{h} = \frac{1}{2Nu_0(Ra)}. \tag{2.1}$$

From theoretical considerations, Kraichnan (1962) derived the $Ra$-dependent Nusselt function $Nu_0$ for two distinct regimes of convection.

### 2.1. *Classical regime*

The first regime called classical is entirely characterized by a constant Rayleigh number for each boundary layer as:

$$\frac{g\alpha \Delta T \delta_{th}^3}{2\nu\kappa} = Ra^*. \tag{2.2}$$

Using (2.1) and (2.2), we obtain for the classical regime:

$$Nu_0^{\mathcal{C}} = \left(\frac{Ra}{2^4 Ra^*}\right)^{1/3}. \tag{2.3}$$

### 2.2. *Ultimate regime*

For very large Rayleigh numbers, the thermal boundary layers observed in the case of the classical regime can be destabilized and Kraichnan (1962) assumed that they could

become similar to the velocity boundary layers observed in the case of a fully developed mean shear flow. This ultimate regime is then characterized by a constant but Prandtl-dependent Péclet number for each thermal boundary layer:

$$\frac{v_0^* \delta_{th}}{\kappa} = Pe^*(Pr), \tag{2.4}$$

where $\kappa = \lambda/(\rho c_p)$ is the thermal diffusivity of the fluid. For small Prandtl numbers, the thickness of the viscous sublayer is smaller than $\delta_{th}$ leading to a constant Péclet number $Pe^* = Pe^*_{Pr\to 0}$. On the contrary, at moderate $Pr$ numbers, $Pe^*$ varies as $\sqrt{Pr}$ since $Pe^* = \sqrt{Pe^*_{Pr\to 0} Re_s Pr}$, where $Re_s$ is the characteristic Reynolds number for the top of the viscous sublayer (Kraichnan 1962). The new unknown parameter $v_0^*$ can be interpreted as a friction velocity and measures the rms value of velocity fluctuations at the edge of each boundary layer, similarly to the friction velocity defined in the case of a channel flow. Unlike the classical regime for which the characteristic Rayleigh number $Ra^*$ depends only on $\Delta T$ and $\delta_{th}$, $Pe^*$ is linked to the convective flow in the bulk by the velocity fluctuations $v_0^*$. Thus, determining the Nusselt number for the ultimate regime requires additional assumptions and equations. The parameter $v_0^*$ is an increasing function of the large-scale mean velocity ($U_0$), also called as the wind turbulence. Its corresponding Reynolds number can be written as $Re_0 = U_0 h/(2\nu)$. By analogy with what is well-known for the channel flow, Kraichnan (1962) assumed that $v_0^* \propto U_0/\ln Re_0$. In addition, the wind velocity is obtained by writing that the Richardson number in the bulk flow is of order 1, *i.e.* $Ri = g\alpha(\overline{w'T'})h/U_0^3 \propto 1$. Using the definitions of $Re_0$, $Ra$ and $Nu_0$, this last equation yields to

$$Re_0^3 \propto \frac{Ra Nu_0}{Pr^2}, \tag{2.5}$$

where $Pr = \nu/\kappa$ is the Prandtl number. We can note that (2.5) is valid for both convection regimes. Using (2.1) and (2.5), (2.4) becomes

$$(Re_0^{\mathcal{U}})^2 \ln(Re_0^{\mathcal{U}}) \propto \frac{Ra}{Pr Pe^*}. \tag{2.6}$$

Then, using (2.6), (2.5) gives the Nusselt number for the ultimate regime:

$$Nu_0^{\mathcal{U}} \propto \left(\frac{Pr\, Ra}{(Pe^* \ln Re_0^{\mathcal{U}})^3}\right)^{1/2}. \tag{2.7}$$

For small $Pr$ numbers (typically $Pr < Pe^*_{Pr\to 0}/Re_s$), $Nu_0^{\mathcal{U}} \propto Pr^{1/2} Ra^{1/2}/(\ln Re_0^{\mathcal{U}})^{3/2}$ while for moderate $Pr$ numbers, $Nu_0^{\mathcal{U}} \propto Pr^{-1/4} Ra^{1/2}/(\ln Re_0^{\mathcal{U}})^{3/2}$.

## 3. $Nu$ vs $Ra$ scalings for internal source driven convection

Using the assumptions discussed below, the $Nu$ *vs* $Ra$ scalings presented in the previous section for standard RB experiments are generalized for the modified experiments described in the introduction and in figure 1. The basic assumption is to state that, for high $Ra$ numbers, the dynamical structure of the convective flow is the same in the standard and modified RB experiments. At a constant $Ra$ number, heating in volume produces the same type of thermal boundary layers as those observed in a standard RB cell. The increase in the power of the heating and cooling sources results in an increase in the bulk flow temperature, but the two types of RB experiments are so similar and the mechanisms that control the convective flow are so robust that for both classical and ultimate regimes, the values of $Ra^*$ and $Pe^*$ are identical in both types of RB experiments.

Secondly, in steady state, the equation of heat averaged over an horizontal section can be written as

$$\frac{\mathrm{d}(\overline{w'T'})}{\mathrm{d}z} - \lambda \frac{\mathrm{d}^2\overline{T}}{\mathrm{d}z^2} = q_v(z). \tag{3.1}$$

The internal heating or cooling source is balanced either by convective flux in the bulk flow or by a conductive flux in both boundary layers. Hereafter, only the lower boundary layer will be considered since the upper boundary layer has the same behaviour. In the boundary layer, by neglecting the convective term and using the expression of $q_v(z)$ (see 1.1), (3.1) can be integrated twice to obtain:

$$\overline{T}(z) - T_h = \frac{Qh}{\lambda}\left\{\frac{z^2}{2h^2} - \frac{z}{h} + \frac{l}{h}[1-\exp(-z/l)]\right\}. \tag{3.2}$$

For $z = \delta_{th}$ and using the definition of the Nusselt number (1.2), (3.2) yields to

$$\frac{1}{2Nu} = \frac{\delta_{th}}{h} - \frac{l}{h}[1-\exp(-\delta_{th}/l)]. \tag{3.3}$$

### 3.1. *Classical regime*

In the classical regime, (2.2) yields to

$$\frac{\delta_{th}}{h} = \left(\frac{2Ra^*}{Ra}\right)^{1/3} = \frac{1}{2Nu_0^{\mathcal{C}}}. \tag{3.4}$$

Using (3.4), (3.3) becomes

$$\frac{Nu^{\mathcal{C}}}{Nu_0^{\mathcal{C}}} = \frac{1}{1 - 2\,\tilde{l}\,Nu_0^{\mathcal{C}}\left[1-\exp\left(-\frac{1}{2\,\tilde{l}\,Nu_0^{\mathcal{C}}}\right)\right]}. \tag{3.5}$$

In (3.4) and (3.5), $Nu_0^{\mathcal{C}}$ is the Nusselt number for a standard RB experiment in the classical regime but it also represents the limit of $Nu^{\mathcal{C}}$ when $\tilde{l} = l/h \to 0$. Even if $Nu^{\mathcal{C}}$ depends on both parameters $\tilde{l}$ and $Ra$, Eq. (3.5) shows that the Nusselt ratio $Nu^{\mathcal{C}}/Nu_0^{\mathcal{C}}$ is a function of a single variable that is the product of $\tilde{l}$ and $Nu_0^{\mathcal{C}}$. This is the main result of the present theory and is tested against experimental results in the section 4.

The limits of (3.5) when $\tilde{l} \to 0$ and $\tilde{l}Nu_0^{\mathcal{C}} \gg 1$ are given in Table 1. It can be noted that, when the product of $\tilde{l}$ and $Nu_0^{\mathcal{C}}$ increases from 0 to $\infty$, the $Ra$-dependent Nusselt number ($Nu^{\mathcal{C}}$) increases from a power law of one third to a two thirds, *i.e.* with an exponent greater than 1/2 which characterizes the ultimate regime for a standard RB experiment (Eq. 2.7).

### 3.2. *Ultimate regime*

Unlike the classical regime for which the thickness of the boundary layers depend only on $Ra$ whatever the type of RB experiment considered (see (3.4)), Eq. (2.4) shows that, in the ultimate regime, $\delta_{th}$ depends on the velocity fluctuations in the bulk ($v^*$) and therefore on the thermal power injected into the bulk flow. Assuming as before that $v^* \propto U/\ln Re$ (Kraichnan 1962), (2.4) becomes for a modified RB experiment

$$\frac{\delta_{th}}{h} = \frac{Pe^*}{Pr}\frac{\ln(Re^{\mathcal{U}})}{Re^{\mathcal{U}}} = \frac{(\delta_{th})_0}{h}\frac{Re_0^{\mathcal{U}}}{\ln(Re_0^{\mathcal{U}})}\frac{\ln(Re^{\mathcal{U}})}{Re^{\mathcal{U}}}. \tag{3.6}$$

For a standard RB experiment, $(\delta_{th})_0$ is given by (2.1) and thus (3.6) becomes

$$\frac{\delta_{th}}{h} = \frac{1}{2Nu_0^{\mathcal{U}}}\frac{Re_0^{\mathcal{U}}}{Re^{\mathcal{U}}}\left[1 + \frac{\ln(Re^{\mathcal{U}}/Re_0^{\mathcal{U}})}{\ln(Re_0^{\mathcal{U}})}\right]. \tag{3.7}$$

| | Classical regime (Eq. 3.5) | Ultimate regime (Eq. 3.9) |
|---|---|---|
| $\tilde{l} \to 0$ | $Nu^{\mathcal{C}} = Nu_0^{\mathcal{C}}\,(1+2\,\tilde{l}\,Nu_0^{\mathcal{C}})$<br>$= \left(\frac{Ra}{64Ra^*}\right)^{\frac{1}{3}}\left[1+\tilde{l}\left(\frac{Ra}{2Ra^*}\right)^{\frac{1}{3}}\right]$ | $Nu^{\mathcal{U}} = Nu_0^{\mathcal{U}}\,\left(1+3\,\tilde{l}\,Nu_0^{\mathcal{U}}\right)$<br>$\propto (C_0^{\mathcal{U}}Ra)^{\frac{1}{2}}\left[1+3\,\tilde{l}\,(C_0^{\mathcal{U}}Ra)^{\frac{1}{2}}\right]$ |
| $\tilde{l}\,Nu_0 \gg 1$ | $Nu^{\mathcal{C}} = 4\,\tilde{l}\,(Nu_0^{\mathcal{C}})^2$<br>$= \tilde{l}\,\left(\frac{Ra}{2Ra^*}\right)^{\frac{2}{3}}$ | $Nu^{\mathcal{U}} = (\frac{2}{1+\alpha})^6\,\tilde{l}^3\,(Nu_0^{\mathcal{U}})^4$<br>$\propto (\frac{2}{1+\alpha})^6\,\tilde{l}^3\,(C_0^{\mathcal{U}}\,Ra)^2$ |

TABLE 1. Limits when $\tilde{l} \to 0$ and $\tilde{l}\,Nu_0 \gg 1$ of the Nusselt number for a modified RB experiment and for the two investigated regimes of convection. For the ultimate regime, $\alpha = \ln(Nu^{\mathcal{U}}/Nu_0^{\mathcal{U}})/(3\ln Re_0^{\mathcal{U}})$ in (3.9) and $C_0^{\mathcal{U}} = Pr/(Pe^*\ln Re_0^{\mathcal{U}})^3$.

As assumed previously for standard RB experiments, the Richardson number in the bulk flow is taken of order 1 *i.e.* $Ri = g\alpha(\overline{w'T'})h/U^3 = g\alpha\kappa Qh/(\lambda U^3) \propto 1$ yielding to $Re^3 \propto RaNu/Pr^2$, similarly to (2.5). Therefore, at constant Rayleigh number, the ratio of the Reynolds numbers for standard and modified RB experiments is proportionnal to the one-third power law of the ratio of the Nusselt numbers

$$\frac{Re}{Re_0} = \left(\frac{Nu}{Nu_0}\right)^{1/3}. \tag{3.8}$$

Furthermore, (3.8) is valid both for ultimate and classical regimes of convection. Using (3.7) and (3.8), (3.3) can be written as

$$\mathcal{N}^2 = \frac{1}{1+\alpha-2\tilde{l}Nu_0^{\mathcal{U}}\mathcal{N}\left[1-\exp\left(-\frac{1+\alpha}{2\tilde{l}Nu_0^{\mathcal{U}}\mathcal{N}}\right)\right]}, \tag{3.9}$$

where $\mathcal{N} = (Nu^{\mathcal{U}}/Nu_0^{\mathcal{U}})^{1/3}$ and $\alpha = \ln\mathcal{N}/\ln Re_0^{\mathcal{U}}$.

In the ultimate regime and similarly to the classical regime case, the ratio $Nu^{\mathcal{U}}/Nu_0^{\mathcal{U}}$ is a function of the product $\tilde{l} \times Nu_0^{\mathcal{U}}$. However, $\alpha$ also depends on the Rayleigh number through the Reynolds number $Re_0^{\mathcal{U}}$. When $\tilde{l} \to 0$, $\alpha \approx 0$ since on the one hand $\mathcal{N} \to 1$ and on the other Reynolds numbers $Re_0^{\mathcal{U}}$ must be large enough to reach the ultimate regime. The limit of (3.9) when $\tilde{l} \to 0$ is then given in Table 1. For large values of $\tilde{l}$, (3.9) can be solved numerically for each chosen couple ($Ra$,$\tilde{l}$) to obtain $\mathcal{N}$ and then $Nu^{\mathcal{U}}$. At high $Nu_0^{\mathcal{U}}$ or else at very high Rayleigh numbers, $Nu^{\mathcal{U}}$ scales asymptotically as $Ra^2$ *i.e.* with an exponent 2 well above 1/2 (see Table 1).

## 4. Comparison with experimental results

The predictions of this theoretical approach can be tested thanks to the recent experimental investigation of Lepot *et al.* (2018); Bouillaut *et al.* (2019). The measurements cover a range of $4 \times 10^6$ to $4 \times 10^9$ for $Ra$ and $10^{-4}$ to 0.1 for $\tilde{l}$. Here, the Rayleigh and Nusselt numbers are defined using $\Delta T = 2(T_h - T_b)$, where $T_h$ and $T_b$ are the measured temperature of the lower plate and the bulk flow, respectively. Hence, there is a factor 2 for $Ra$ (and a factor 1/2 for $Nu$) by comparing the figures from Lepot *et al.* (2018); Bouillaut *et al.* (2019) and with those presented here.

The theory presented previously shows that Nusselt numbers for various $\tilde{l}$ should

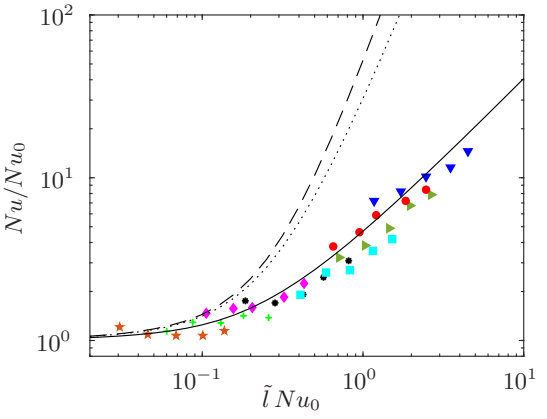


FIGURE 2. Compensated Nusselt for a modified RB experiment as a function of $\tilde{l}Nu_0$, in the classical regime (solid line, Eq. 3.5, no adjustable parameter) and in the ultimate regime (dotted and dashed lines, (3.9) with $Re_0^{\mathcal{U}} = 1000$ and $Re_0^{\mathcal{U}} = 10^{10}$, respectively). Also shown: experiments from Bouillaut *et al.* (2019) with $\tilde{l} = 0.0015$ ($\star$), $\tilde{l} = 0.003$ ($+$), $\tilde{l} = 0.006$ ($\diamond$), $\tilde{l} = 0.0012$ ($*$), $\tilde{l} = 0.0024$ ($\square$), $\tilde{l} = 0.048$ ($\triangleright$), $\tilde{l} = 0.05$ ($\circ$), $\tilde{l} = 0.096$ ($\nabla$).

collapse on a single curve by plotting the ratio of the Nusselt numbers for modified and standard RB experiments ($Nu/Nu_0$) as a function of the product of $\tilde{l}$ and $Nu_0$. In figure 2, the solid line represents the curve given by (3.5) for the classical regime while the two upper lines represent the ultimate regime (Eq. 3.9) for two fixed Reynolds numbers: $Re_0^{\mathcal{U}} = 1000$ (dotted line) and $Re_0^{\mathcal{U}} = 10^{10}$ (dashed line). Indeed, for the ultimate regime, the Nusselt ratio depends slightly on $Re_0^{\mathcal{U}}$ through the $Re_0^{\mathcal{U}}$-dependent coefficient $\alpha$. However, the two curves for the ultimate regime are actually quite close to each other. The experimental results from Bouillaut *et al.* (2019) are also plotted in Fig. 2, using the Nusselt numbers obtained for $\tilde{l} = 10^{-4}$ as a reference for $Nu_0$. Two main conclusions can immediately be drawn. First, the experimental data obtained for various $\tilde{l}$ collapses on the same curve and secondly this curve is given by (3.5) with a fairly good accuracy. This validates the present theoretical approach and also shows that the ultimate regime was not reached in previous experiments.

In figure 3, the Nusselt ratio is plotted as a function of $Nu_0$ for $\tilde{l} = 0.006$ and $\tilde{l} = 0.05$. In the classical regime (solid lines), as $Nu_0^{\mathcal{C}} \propto Ra^{1/3}$, $Nu^{\mathcal{C}}$ varies as $Ra^{1/3}$ when $\tilde{l} \to 0$ or when $Ra$ is low, while $Nu^{\mathcal{C}}$ varies as $Ra^{2/3}$ when $\tilde{l} \times Ra^{1/3}$ is quite high. Thus, the scaling $Nu^{\mathcal{C}} \propto Ra^{1/2}$ can only be observed for a limited range of $Ra$ for each $\tilde{l}$ considered. Bouillaut *et al.* (2019) have proposed to represent the experimental data considering the product of $Nu$ and $\tilde{l}^2$ as a function of the product of $Ra$ and $\tilde{l}^6$ (see Fig. 4). The model presented here shows that, in this representation, the experimental data can only collapse on a single curve if both the range of $Ra$ is relatively small and this range is the same for all the $\tilde{l}$ investigated. On the contrary, the model for the classical regime (3.5) predicts that $Nu^{\mathcal{C}}\,\tilde{l}$ depends only on $Nu_0^{\mathcal{C}}\,\tilde{l}$ or only on $Ra\,\tilde{l}^3$ with assuming $Nu_0^{\mathcal{C}} \propto Ra^{1/3}$ (Eq. 2.3). Besides, in this representation, the curve is given by (3.5) and without any adjustable parameter.

In the ultimate regime, $Nu^{\mathcal{U}}(\tilde{l}, Ra)$ also depends on the parameter $Pe^*$ (or rather on $Pe^*/Pr$), at least when $\alpha$ cannot be neglected. Indeed, $\alpha$ is proportionnal to $\ln Re_0^{\mathcal{U}}$ and using (2.5) and (2.6) we have

$$\frac{\ln Re_0^{\mathcal{U}}}{Re_0^{\mathcal{U}}} \propto \frac{Pr}{Pe^* Nu_0^{\mathcal{U}}}. \tag{4.1}$$

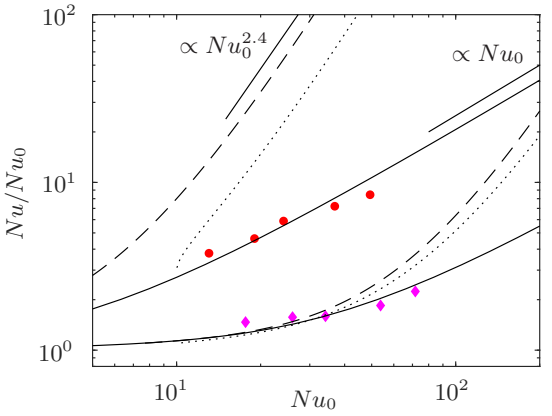


FIGURE 3. Compensated Nusselt as a function of $Nu_0$ for two fixed $\tilde{l}$, in the classical regime (solid lines, Eq. (3.5), no adjustable parameter) and in the ultimate regime (dashed and dotted lines, Eq. (3.9) and using (4.1)). Symbols: experiments from Bouillaut *et al.* (2019). Lower lines and purple diamonds: $\tilde{l} = 0.006$. Upper lines and red circles: $\tilde{l} = 0.05$. For the ultimate regime, the parameter $(Nu_0^{\mathcal{U}})_{\min} = Pr\, e^1/Pe^*$ is fixed to 0.1 (dashed lines) or else 10 (dotted lines).

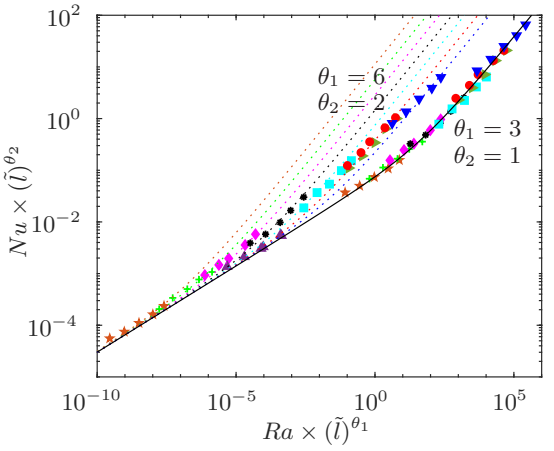


FIGURE 4. Comparison of the scaling proposed by Bouillaut *et al.* (2019) and the model described in section 3. Upper dotted lines (Eq. 3.5) and upper symbols: $Nu\,\tilde{l}^2$ *vs* $Ra\,\tilde{l}^6$. Lower solid line (Eq. (3.5), without adjustable parameter) and lower symbols: $Nu\,\tilde{l}$ *vs* $Ra\,\tilde{l}^3$. Symbols as in Fig. 2.

Equation (4.1) shows that $Nu_0^{\mathcal{U}}$ must be greater than a minimum value $(Nu_0^{\mathcal{U}})_{\min} = Pr\, e^1/Pe^*$. Using (4.1), the Nusselt ratio is plotted as a function of $Nu_0$ in Fig. 3 for $\tilde{l} = 0.006$ and $\tilde{l} = 0.05$, and for two values of the parameter $(Nu_0^{\mathcal{U}})_{\min}$ (0.1 and 10). For the greater value of $\tilde{l}$, $Nu^{\mathcal{U}}/Nu_0^{\mathcal{U}}$ seems to vary as $(Nu_0^{\mathcal{U}})^{2.4}$ yielding to $Nu^{\mathcal{U}} \propto (Nu_0^{\mathcal{U}})^{3.4}$ and showing that the asymptotic behaviour $Nu^{\mathcal{U}} \propto (Nu_0^{\mathcal{U}})^4 \propto Ra^2$ can only be reached for very high Rayleigh numbers for which $\alpha$ tends towards a constant value. Finally, to our knowledge, no experimental or numerical study of a modified RB cell has been able to reach a Rayleigh number high enough to test this model in the ultimate regime.

## 5. Conclusion

A simple model without adjustable parameter has been described here to predict the evolution of the Nusselt number of a modified RB experiment as a function of the two

variables $Ra$ and $l/H$, where $l$ is the heating length near the lower plate. The model is based on the theoretical study of Kraichnan (1962) for which two convection regimes are considered: the classical regime giving a scaling law as $Nu \propto Ra^{1/3}$ and the ultimate regime, achievable only at very high $Ra$, with $Nu \propto Ra^{1/2}$. For a modified RB experiment and in the classical regime, an analytical equation (3.5) has been given for $Nu^{\mathcal{C}}(Ra, l/H)$ and this prediction has been tested against recent experimental results. An excellent agreement has been observed between the model and the experiments, even if for a standard RB cell, the exponent 1/3 is barely observed experimentally or numerically and the exponent varies from 0.29 to 0.32 in the range of $Ra$ between $10^6$ and $10^{10}$. An analytical equation (3.9) has been also given for the ultimate regime giving the ratio of $Nu^{\mathcal{U}}/Nu_0^{\mathcal{U}}$ without adjustable parameter, regardless of the value of the transition Rayleigh between the two convection regimes. Finally, the model predicts that the Nusselt number behaves asymptotically as $Ra^{2/3}$ for the classical regime while it scales as $Ra^2$ when $Ra$ tends towards infinity, and this prediction is of major interest for geophysical and astrophysical flows where convection is driven by internal heat sources.

## Acknowledgements

Bernard Castaing is gratefully thanked for his suggestions and the review of the article.

## REFERENCES

Ahlers, G., Grossmann, S. & Lohse, D. 2009 Heat transfer and large scale dynamics in turbulent Rayleigh-Bénard convection. *Rev. Mod. Phys.* **81**, 503–537.

Bouillaut, V., Lepot, S., Aumaître, S. & Gallet, B. 2019 Transition to the ultimate regime in a radiatively driven convection experiment. *J. Fluid Mech.* **861**, R5.

Chavanne, X., Chillà, F., Castaing, B., Hébral, B., Chabaud, B. & Chaussy, J. 1997 Observation of the ultimate regime in Rayleigh-Bénard convection. *Phys. Rev. Lett.* **79**, 3648–3651.

Chillà, F & Schumacher, J. 2012 New perspectives in turbulent Rayleigh-Bénard convection. *Eur. Phys. J. E* **35**, 58.

Doering, C. R. 2019 Thermal forcing and classical and ultimate regimes of Rayleigh-Bénard convection. *J. Fluid Mech.* **868**, 1–4.

Goluskin, D. 2015 *Internally Heated Convection and Rayleigh-Bénard Convection*. Springer.

Goluskin, D. & van der Poel, E. P. 2016 Penetrative internally heated convection in two and three dimensions. *J. Fluid Mech.* **791**, R6.

Kraichnan, R. H. 1962 Turbulent thermal convection at arbitrary Prandtl number. *Phys. Fluids* **5** (11), 1374–1389.

Kulacki, F. A. & Goldstein, R. J. 1972 Thermal convection in a horizontal fluid layer with uniform volumetric energy sources. *J. Fluid Mech.* **55** (2), 271–287.

Lepot, S., Aumaître, S. & Gallet, B. 2018 Radiative heating achieves the ultimate regime of thermal convection. *Proc. Natl Acad. Sci. USA* **115**, 8937–8941.

Qiu, X.-L., Xia, K.-Q. & Tong, P. 2005 Experimental study of velocity boundary layer near a rough conducting surface in turbulent natural convection. *J. Turbul.* **6**, 30.

Roche, P.-E., Castaing, B., Chabaud, B. & Hébral, B. 2001 Observation of the 1/2 power law in Rayleigh-Bénard convection. *Phys. Rev. E* **63** (4), 045303.

Shen, Y., Tong, P. & Xia, K.-Q. 1996 Turbulent convection over rough surfaces. *Phys. Rev. Lett.* **76**, 908–911.

Siggia, E. D. 1994 High rayleigh number convection. *Ann. Rev. Fluid Mech.* **26** (1), 137–168.

Stringano, G., Pascazio, G. & Verzicco, R. 2006 Turbulent thermal convection over grooved plates. *J. Fluid Mech.* **557**, 307–336.

Tisserand, J.-C., Creyssels, M., Gasteuil, Y., Pabiou, H., Gibert, M., Castaing, B. & Chillà, F. 2011 Comparison between rough and smooth plates within the same Rayleigh-Bénard cell. *Phys. Fluids* **23** (1), 015105.